Fırat Üniversitesi Müh. Bil. Dergisi
38(1), 201-212, 2026

Araştırma Makalesi
https://doi.org/10.35234/fumbd.1790146

Numerical Assessment of Multi-Cell Thin-Walled Beams under Three-Point Bending for Automotive Safety

Mehmet KOPAR[1*], Medeni SÖMER[2], Ali ARI[3]

[1] Department of Mechanical and Metal Technologies, Weapon Industry Technician Program, Vocational School, Ostim Technical University, Ankara, Turkey

[2] Department of Electrical and Energy, Hybrid and Electric Vehicles Technology Program, Hitit University, Corum, Turkey

[3] Department of Mechanical and Metal Technologies, Weapon Industry Technician Program, Vocational School, Ostim Technical University, Ankara, Turkey

[*1] mehmet.kopar@ostimteknik.edu.tr, [2] medenisomer@hitit.edu.tr, [3] ali.ari@ostimteknik.edu.tr

(Geliş/Received: 24/09/2025; Kabul/Accepted: 30/12/2025)

Abstract: In this study, the impact strength of automotive side door beams reinforced with multi-cell thin-walled structures was investigated under three-point bending loads. Six different configurations (cylindrical and square outer geometries with 3, 4, and 5 inner cells) made of AA6063-T1 aluminum alloy were analyzed using the finite element method. The models developed in HyperMesh were validated with the experimental data of Zhang and Fu, and an error of less than 1.1% was achieved. The results revealed that increasing the number of inner cells significantly increased the energy absorption, average crushing force, and specific energy absorption. The square-profile K5 design achieved the best performance with 0.1617 kJ EA and 0.885 kJ/kg SEA, outperforming its cylindrical counterpart (S5) by 43% and 13%, respectively. The square geometries also exhibited a 69% higher peak crushing force due to their superior vertical load-carrying behavior. The findings indicate that multicellular thin-walled structures offer significant advantages over traditional single-cell designs, providing up to 27-42% improvement in crash performance and are an effective design strategy for lightweight automotive safety components.

Keywords: Three-point bending test, energy absorption, crashworthiness, finite element analysis (FEA).

Otomotiv Güvenliği Açısından Çok Hücreli İnce Duvarlı Kirişlerin Üç Nokta Bükülme Altında Sayısal Değerlendirilmesi

Öz: Bu çalışmada, çok hücreli ince duvarlı yapılarla güçlendirilmiş otomotiv yan kapı kirişlerinin üç noktalı bükülme yükleri altında çarpma dayanıklılığı araştırılmıştır. AA6063-T1 alüminyum alaşımından yapılmış altı farklı konfigürasyon (3, 4 ve 5 iç hücreli silindirik ve kare dış geometriler) sonlu elemanlar yöntemi kullanılarak analiz edilmiştir. HyperMesh'te geliştirilen modeller, Zhang ve Fu'nun deneysel verileriyle doğrulanmış ve %1,1'den daha az hata elde edilmiştir. Sonuçlar, iç hücrelerin sayısının arttırılmasının enerji emilimini, ortalama kırma kuvvetini ve spesifik enerji emilimini önemli ölçüde arttırdığını ortaya çıkarmıştır. Kare profilli K5 tasarımı, 0,1617 kJ EA ve 0,885 kJ/kg SEA ile en iyi performansı elde ederek silindirik muadilini (S5) sırasıyla % 43 ve %13 oranında daha iyi değerlere sahip olduğu belirlenmiştir. Kare geometriler ayrıca üstün dikey yük taşıma davranışı nedeniyle % 69 daha yüksek tepe kırma kuvveti göstermiştir. Bulgular, çok hücreli güçlendirilmiş kare yapıların, geleneksel tek hücreli tasarımlara göre önemli avantajlar sunduğunu, çarpışma performansında %27-42'ye kadar iyileşme sağladığını ve hafif otomotiv güvenlik bileşenleri için etkili bir tasarım stratejisi olduğu belirlenmiştir.

Anahtar Kelimeler: Üç nokta eğme testi, enerji emilimi, çarpışma dayanıklılığı, sonlu elemanlar analizi (FEA).

1. Introduction

Engineering design paradigms center around the 21st century triad of material proportions, density, sustainability and durability [1]. For this reason, structures with thin-walled structures, despite their low density, exhibit superior lightness, high strength and energy properties, and due to their ability to withstand the same; It has a wide application potential in many products, from automotive to aviation, from construction to defense industry. Especially the need for lightweight and high impact resistant designs and the usage rate of these structures are rapidly increasing [2-4].

In recent years, automotive economy performance, safety and fuel change have been continuously upgraded and affordability, lightweight design and flexibility have been highlighted [5-7]. Within the framework of these

* Sorumlu yazar: mehmet.kopar@ostimteknik.edu.tr. Yazarların ORCID numarası: [1] 0000 0001 7347 4192, [2] 0000 0003 4411 3309, [3] 0000-0003-2702-2982

needs, the performance and preference of walled structures has become a frequent choice in electrical designs. These types of structures are elements with open or closed sections, which can be produced especially with metal or composite materials, with at least one system being very low in the wall gap. Despite their low relative dissipation, they show high rigidity and excellent energy absorption properties, and the diversity and safety of these structures are critical, making them widely sold in the automotive and aviation sectors [8].

In automotive; Passive safety elements such as pillar reinforcements, bumper beams and especially the side door beam have an important and vital role in protecting the integrity of the passenger cabin during a collision [8]. By preventing the door from collapsing inwards during an impact, side door beams not only reduce the acceleration experienced by the driver and passengers, but also help dampen the resulting collision force in a controlled manner. Therefore, it is aimed to increase the energy absorption capacity of structural designs by intensifying studies on different cross-section geometries, cell configurations and material combinations [9, 10].

In addition to traditional thin-walled structures [11, 12]; The use of multi-cell, foam-filled or hybrid structures, porous [13, 14], biomimetic [15, 16] and multi-cell [17, 18] structures significantly increase impact resistance and make collapse modes more predictable. In most studies in the literature, polygonal and circular sections are analyzed comparatively; It has been shown that parameters such as number of cells, wall thickness, and material type directly affect energy absorption performance. It is known that especially three-, four- or five-cell structures increase crash resistance and offer more stable deformation modes than single-wall systems [19].

Energy absorption performances of thin-walled structures; It varies significantly depending on section geometry, wall thickness, material type, length/width ratio and loading conditions [20, 21]. For example, studies on tubes with circular, square, rectangular, hexagonal and polygonal cross-sections have shown that each geometry has different advantages [22]. While circular tubes provide continuous and stable energy absorption with the progressive axial folding mode; Polygonal cross-section tubes can offer higher rigidity during folding [23]. But while increasing the number of corners generally increases folding stability, it may also affect the forces occurring at the first impact [24].

Not only axial loading of thin-walled structures, but also complex loading scenarios such as bending and torsion can significantly affect the performance of these structures [25]. Three-point bending loading is frequently preferred as a test method representing real crash scenarios to evaluate the stiffness, energy absorption capacity and deformation mechanisms of the structure [26]. Deformation behavior of structures under bending loads; It is shaped by mechanisms such as local buckling, plastic hinge formation and crustal collapse. In addition, manufacturing-related initial defects and geometric irregularities also play a determining role in the mechanical response of the structure. For this reason, finite element analyzes calibrated with experimental studies are considered an indispensable tool to obtain realistic and reliable results [27, 28].

Current literature highlights various strategies to improve the energy dissipation performance of thin-walled structures. Halis and Altın (2024) [29] investigated the use of E-glass/PET199 composite material in seven different thin-walled beam geometries and determined that this composite improved the CFE value by 2.32% while maintaining the SEA value at the same level as AA6063-T1 alloy (1.08 kJ/kg). Albak (2022) [30] investigated the effects of parameters such as cell number and reinforcement orientation in multi-cell thin-walled tubes and showed that W1L1 and W1L1S1 tubes optimized by COPRAS and MOGA methods reduced the PCF values by 13.1–15.4% while maintaining the SEA value. Similarly, Zheng et al. (2021) [31] reported that axial restraint can increase energy dissipation by a factor of 2.5–3, and tubes with stiffeners placed parallel to the load direction (MT-Y0Zn) exhibited better performance. Gliszczyński and Czechowski (2017) [32] emphasized that the layer arrangement in GFRP laminated channel beams critically affects the flexural strength, and symmetric configurations such as [0/−45/45/90]S optimize the performance. Zhang and Fu (2023) [33] stated that the maximum moment does not always occur in the mid-span region in three-point bending tests, suggesting that existing theoretical models should be revised. Huang and Zhang (2018) [34] revealed the inadequacy of the Kecman model for three-point bending and proposed a new theoretical method that emphasizes the critical role of geometric parameters. Huang et al. (2021) [35] showed that the SEA value can be increased up to 70.6% by optimizing the CFRP layout in Al/CFRP hybrid beams, and that local collapses improve energy absorption, especially in off-center impacts. Kim et al. (2013) [36], on the other hand, stated that the SEA value of Al/CFRP beams with [0/+45°/90°/−45°]n layer arrangement increased by 29.6%, but this improvement was not directly related to the damage area, drawing attention to the design flexibility of hybrid materials. Tang et al. [37] numerically investigated multi-cell circular tubes consisting of concentric rings radially connected by multiple networks, and determined that the wall thickness and the number of cells in the circumferential and radial directions significantly affect the energy absorption performance; double-layer multi-cell tubes achieved the highest SEA value. Chen et al. [38] proposed four hybrid multi-cell thin-walled structures with circular and square cross-sections and reported that the dimensions of the outer tubes and the wall thickness have a decisive effect on

energy dissipation. All these studies jointly emphasize the critical importance of material selection, geometric optimization, and loading conditions in improving energy dissipation performance.

In this study, six different side door beams with square and circular sections reinforced with multi-cell internal structures were designed to increase the crash resistance of traditional single-walled thin-walled structures. All models are 370 mm long and 1 mm wall thick, and the internal structures are optimized with three, four and five cells. Cell diameters and center circle dimensions were kept constant, thus enabling comparative analysis. These structures, modeled using AA6063-T1 aluminum alloy, were subjected to three-point bending loading; Performance criteria such as maximum collision force (PCF), average collision force (MCF), energy absorption (EA), specific energy absorption (SEA) and efficiency were evaluated. Model validation was carried out with experimentally obtained data by Zhang and Fu, and the results were found to be compatible with a maximum error rate of 1.1%. In this context, finite element modeling provided reliable results and all analyzes were carried out on this validated model. The results obtained show that increasing the number of inner cells positively affects EA, MCF and SEA values; It shows that square-section structures have a higher load-carrying capacity compared to circular-section structures. Especially the building coded K5 offers the highest value in terms of SEA; The structure coded S5 also showed a similarly high energy absorption performance. The difference in folding behavior depending on the geometry clearly reveals the effect of the outer section form on crash resistance. As a result, it appears that thin-walled side door beams optimized with multi-cell internal reinforcements offer significant advantages over conventional designs in terms of both specific energy absorption and collapse behavior. These findings will shed light on future studies on performance optimization of automotive safety structures.

2. Side Door Beam Design

Scientists have conducted many studies in recent years on the development of passive and active safety systems to ensure passenger safety in the automotive industry. Side door bars, one of the most critical components of passive safety systems used in the automotive industry, provide passenger safety by preventing the door from moving inward by absorbing the energy generated during a crash. It aims to enhance energy absorption performance by utilizing various cross-sections and geometries in the design of side door bars. In addition to traditional materials such as aluminum, steel, and magnesium, composite materials are now being used as materials for side door bars. Additionally, thanks to the development of additive manufacturing technologies, it is now possible to produce door bars with complex geometries. Figure 1 shows the location of the side door bar on the automotive door.

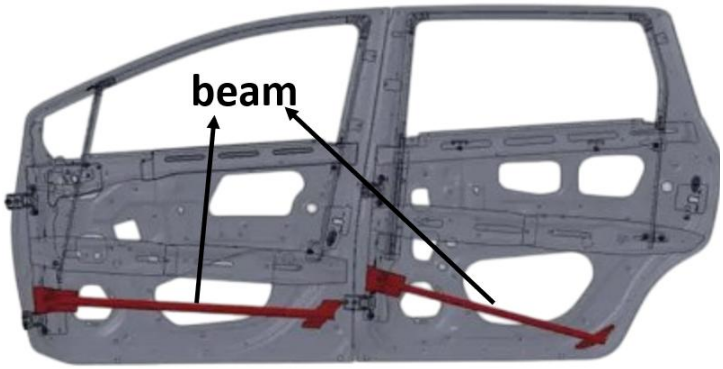

Figure 1. Illustration of the position of the side door bars on the vehicle [39]

This study designed six different multi-cellular automotive side doors with cylindrical and square exterior as shown in Figure 2. The codes of the automotive side door bars are given in Figure 2. All door bars are designed with a wall thickness of 1 mm and a length of 370 mm. When the designs given in Figure 2 are examined, the inner parts of the hollow square and cylinder door bars are reinforced with multi-cellular structures, three, four, and five, respectively. Here, the diameters of the circles in the inner part are designed to be 7 mm, and the diameter of the circle in the center, where the cells are placed, is intended to be 17 mm. In all designs, multi-cellular structures were designed by fixing them at the center points of the square and cylinder structures.

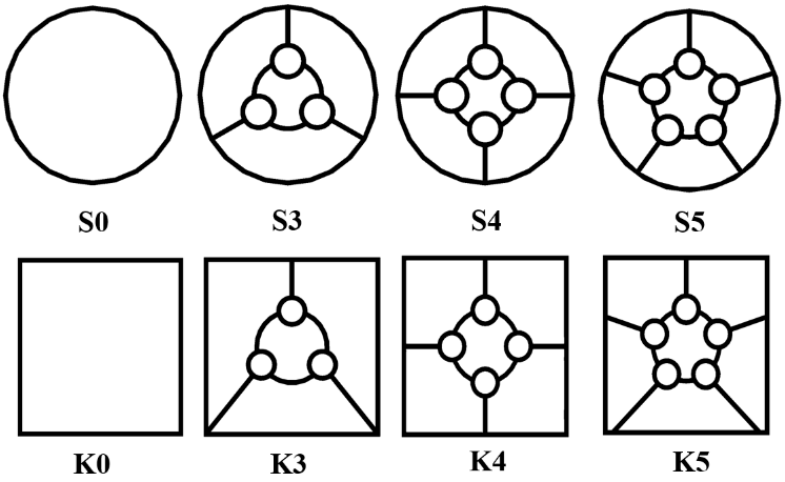

Figure 2. Automotive side door bar designs and nomenclature

3. Finite Element Model

This section analyzes the side door bars designed as described in Section 2. However, firstly, the validations of the tests performed in Zhang and Fu's [40] study were carried out, and the data of the validated analyses with small error rates were used in this study. In their study, Zhang and Fu produced multi-cell structures by reinforcing an aluminum structure with dimensions of 32 x 32 x 370 mm and a wall thickness of 0.95 mm, using 1.05 mm thick aluminum, as shown in Figure 3(a). Then, they performed three-point bending tests on the aluminum structures, as shown in Figure 3(b), with a 320 mm distance between the supports and 24 mm between the indenter and support diameters, and examined the energy absorption performance of the structures.

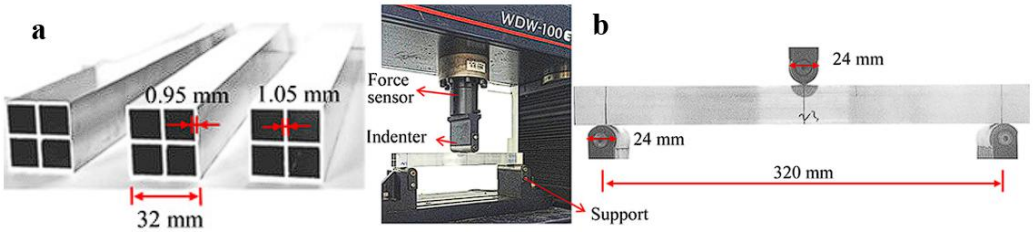

Figure 3. Three-point flexure test visuals: a) structure dimensions, b) test procedure [40]

Zhang and Fu performed tensile tests at a speed of 1 mm/s, in accordance with the ASTM E8M-04 standard, to determine the mechanical properties of the AA6063-T1 material. They determined the stress-strain values in Table 1 and the mechanical properties in Table 2.

Table 1. True stress-strain relation of AA6063-T1 [40]

Plastic strain	0	0.0112	0.0215	0.0305	0.0393	0.0482	0.0589	0.0756	0.0933
Stress	100	124.7	142.8	156.5	168	178.4	189.5	204.6	218
Plastic strain	0.111	0.129	0.146	0.164	0.184	0.204	0.224	0.250	
Stress	229.3	239.6	248.2	256.4	264.5	271.7	278.4	286	

Table 2. Mechanical properties of AA6063-T1 material [40]

Density	**Young's modulus**	**Poisson's ratio**	**Yield stress**	**Ultimate stress**
ρ= 2700 kg•m^{-3}	E = 68.9 GPa	ν= 0.33	σ_y = 100 MPa	σ_u = 222 MPa

Zhang and Fu also performed validation using the finite element method in their study. In this study, validation was performed using the Hypermesh finite element program under conditions similar to those of the test, as shown in Figure 4. AA6063-T1 material was created using the MAT-36 material found in the Hypermesh program. The support and indenter are rigid materials that prevent deformation during the analysis. The thicknesses of the internal and external structures were determined by using two different shell cards as feature cards. Then a TYPE-7 contact card was established between the indenter, supports, and aluminum. The coefficient of friction between all structures was defined to be 0.3. Finally, a speed of 1 mm/s was determined for the indenter, and analyses were performed.

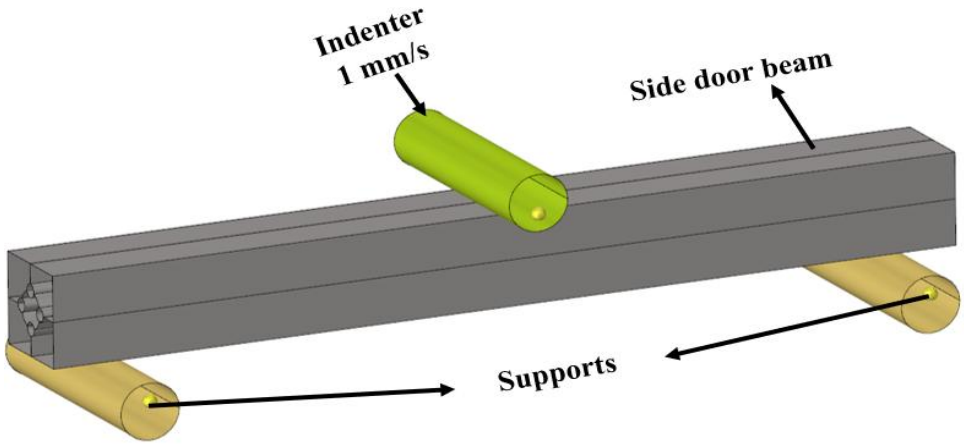

Figure 4. Setting up the finite element analysis

To examine the durability of the side door bars, it is necessary to determine the PCF, MCF, EA, SEA, and efficiency criteria.

The energy absorption (EA) represents the total energy dissipated by the structure during deformation and is calculated using Equation (1) [41];

$$EA = \int_0^d F(x)dx, \tag{1}$$

Where d is the loading distance and $F(x)$ is the instantaneous load amount.

The mean crushing force (MCF) can be obtained using Equation (2) [41].

$$F_{mean} = \frac{EA}{d} \tag{2}$$

The specific energy absorption (SEA), which represents the absorbed energy per unit mass, is calculated according to Equation (3) [41].

$$SEA = \frac{EA}{m} \tag{3}$$

Finally, the crash force efficiency (CFE) is determined using Equation (4) [41].

$$CFE = \frac{F_{mean}}{F_{max}} \tag{4}$$

Figure 5(a) compares the experimental results (black curve) obtained by Zhang and Fu with the numerical validation results from both Zhang and Fu [40] (blue curve) and Kopar, Sömer, and Ari in the current study (red curve). As can be seen, all curves show a rapid initial force increase, followed by a plateau at approximately 2700-3000 N. High agreement was observed between the experimental and numerical results in terms of maximum force

values. However, the validation curve obtained in the current study, similar to the experimental results, exhibits a slight decreasing trend as the displacement progresses. This may be attributed to differences in material modeling and contact conditions.

Figure 5(b-d) shows the relevant test specimen, geometric model, and finite element mesh. Visual comparisons reveal that the generated numerical model agrees with the experimental setup.

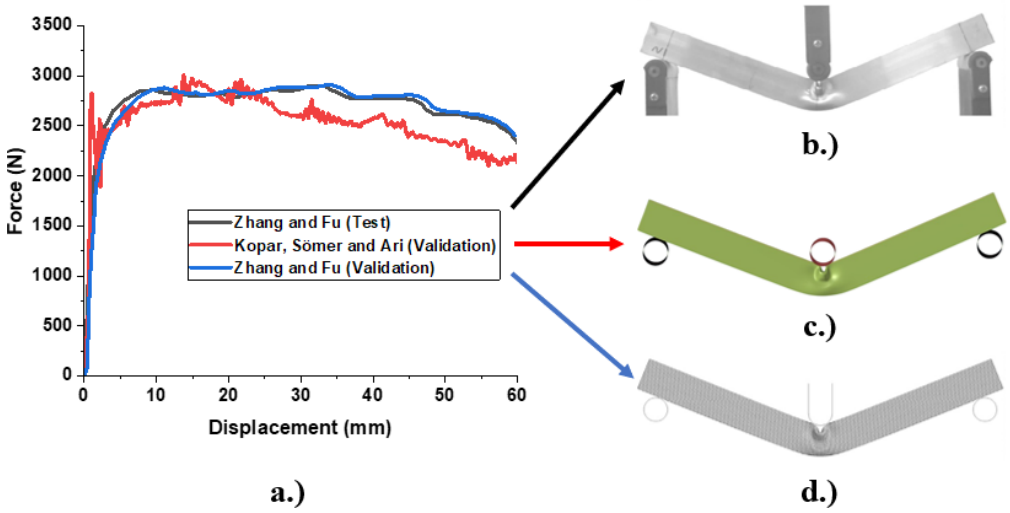

Figure 5. Validation results: a) force-displacement graph, b) Zhang and Fu test bending image[40], c) Kopar, Sömer, and Ari validation bending image, d) Zhang and Fu simulation bending image[40]

Validation simulation data were used to calculate the crash safety parameters of the side door bars using Equations (1-4), and compared with experimental results. The data obtained from the finite element analysis and the results presented in Zhang and Fu's [40] study are provided in Table 3. When the crash criterion values in Table 3 are examined, an error rate of approximately 0.1% was achieved when comparing the test and validation results for SEA. Because the SEA value is the most critical factor in collision and bending analyses, the mesh sensitivity value was also approximated using the SEA value.

Table 3. Comparison of results

	MCF (N)	Displacement (mm)	Mass (kg)	EA (kJ)	SEA (kJ/kg)	SEA Error (%)
Zhang and Fu (Test) [40]	2861	60	0.1830	0.1618	0.884	-
Zhang and Fu (FEA) [40]	-	60	0.1830	0.1648	0.888	0.54
Kopar, Sömer, and Ari (FEA)	2828	60	0.1830	0.1617	0.885	0.1

During the finite element analysis, the unit size of the mesh structure has a significant impact on the results obtained. Therefore, to determine the optimum mesh sizes in the validation phase, analyses were performed with meshes having dimensions of 1 mm, 1.5 mm, 2 mm, 2.5 mm, and 3 mm, and the closest value to Zhang and Fu's [40] study was determined in terms of SEA value. When Figure 6 is examined, it is determined that the optimum mesh size is 1 mm, and all analyses were performed with a mesh size of 1 mm.

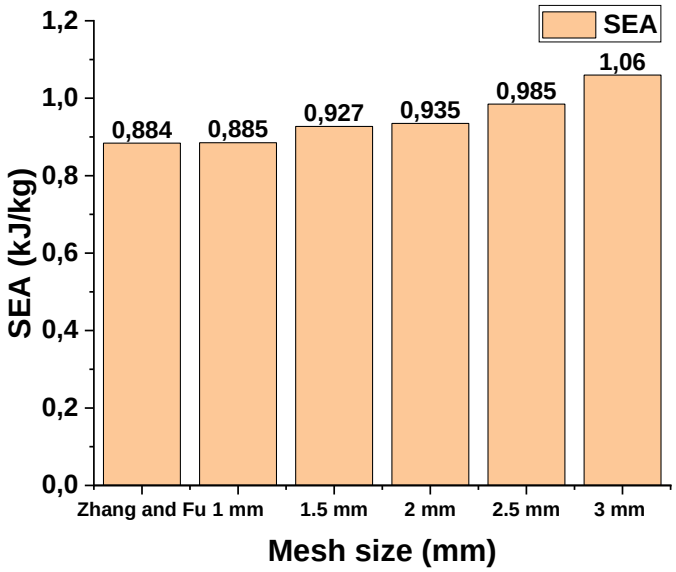

Figure 6. Investigation of the mesh effect in a finite element model

4. Results

Figure 7(a-b) shows the force-displacement graphs obtained from three-point bending analysis. When Figure 7(a) is examined, it is determined that the structure with the maximum PCF value is the side door bar coded S5, which is approximately 4629 N. It is determined that the PCF value of the side door, bar coded S5, is 13% higher than S4, 27% higher than S3, and approximately four times higher than S0. Upon examining Figure 7(b), it is determined that the side door bar, coded K5, has a high PCF value of approximately 6489 N. The PCF value of the side door, bar coded K5, is approximately 16% higher than K4, 27% higher than K3, and 69% higher than K0.

When K and S coded side door bars are compared with each other, it is thought that K coded side door bar designs have a higher PCF value, and the main reason for this is that the square structure meets the force vertically.

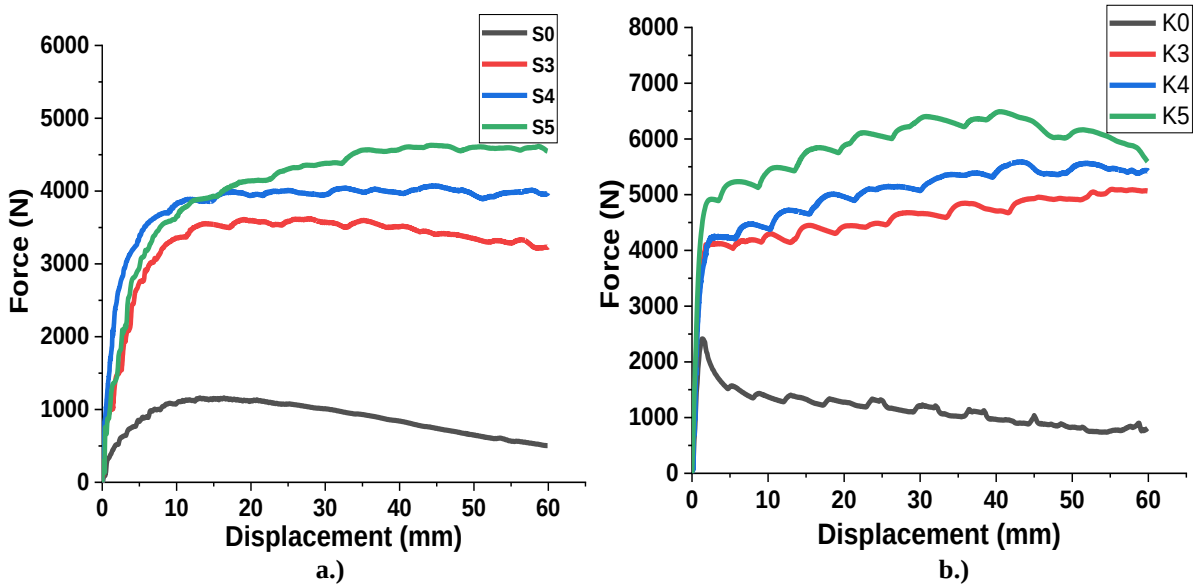

Figure 7. Force-displacement graph obtained as a result of three-point bending analysis of side door bars: a) S-coded structures, b) K-coded structures

Figure 8(a-d) shows the crash performance criterion values calculated using the data obtained after the simulations of all designs. When Figure 8(a) is analyzed, it is determined that the EA value increases in both S-

coded and K-coded side door bars due to the increase in the number of cells in the interior. It was determined that the side door bar with the highest energy absorption was K5 among the K-coded structures, while the side door bar coded S5 among the S-coded structures. It was determined that the door bar with the highest EA value was K5, and it was found to provide approximately 43% higher energy absorption than S5.

When the MCF value given in Figure 8(b) is examined, just like the EA values, an increase was realized due to the increase in the number of cells in the interior. Here, it is determined that the structure with the highest MCF value is S5 among the S-coded designs and K5 among the K-coded designs. It was determined that the K5 design was approximately 42 % higher than the S5. When the SEA values given in Figure 8(c) are analyzed, it is determined that the design coded K5 has the maximum value, approximately 13% higher than S5.

When the crash criteria given in Figure 8 are examined, it is observed that for all values, an increase occurs due to the increase in the number of cells in the inner part. The increase in cell structures here is likely due to increased surface area to meet the force. It was determined that designs with square geometry on the outer parts exhibited higher performance than those with cylindrical geometry. This is likely because the struts on the sides of the square structure are more effective in resisting the force. Figure 8.d shows that the CFE has significantly increased in both S and K coded structures with increased internal cells. Designs coded S0 and K0 were found to have the lowest crash efficiencies due to their cell-less design, with efficiencies of 0.75% and 0.48%, respectively. Due to the increased number of cells in the internal structure of the cylindrical and square-shaped side door bars, crash efficiencies improved by approximately 17% for S5 compared to S0. It was determined that K5 achieved an approximately 88% increase in CFE compared to K0.

K-series side door bars were found to have a higher CFE value than almost all S-series designs due to their load-carrying properties and more stable plastic deformations. The results revealed that the internal cell structure significantly impacted CFE values.

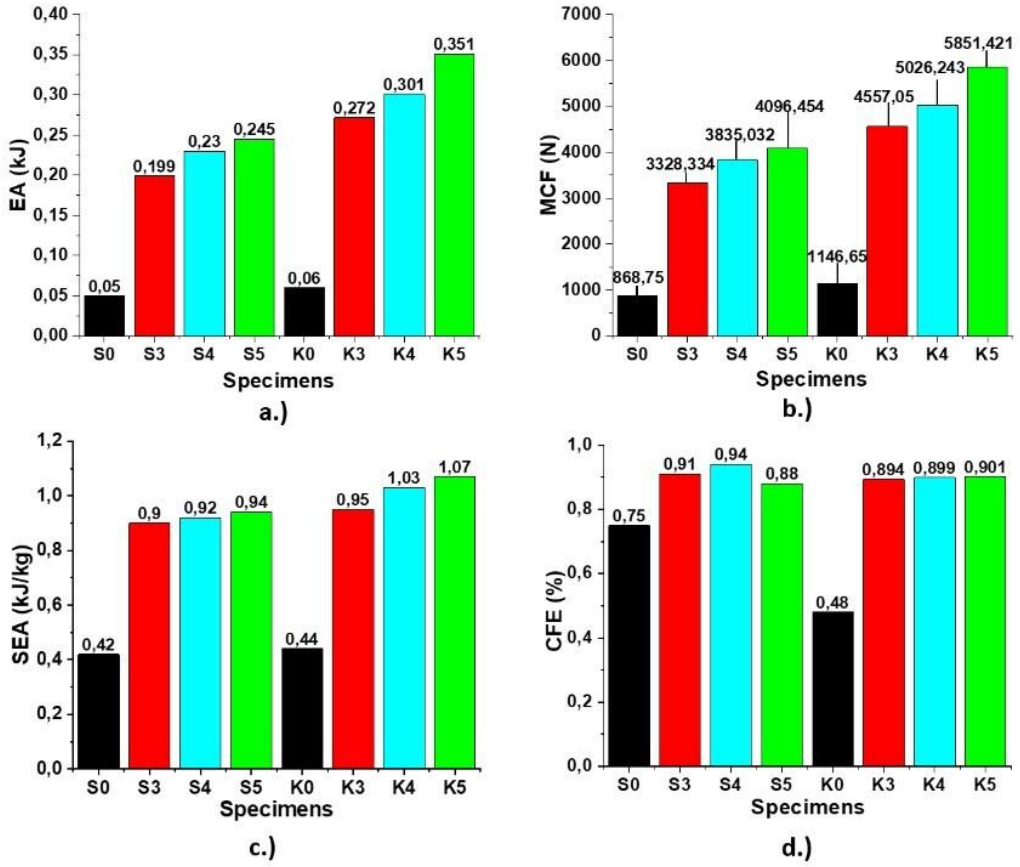

Figure 8. Crash criteria: a) EA, b) MCF, c) SEA, d) CFE

Figure 9(a-b) shows the bending behavior of the S5 and K5 side door bars, which have high crash performance criteria values. Figure 9(a) shows the bending images of the K5 side door bar, which has a five-cell structure on the inside, and when this bending behavior is examined, it is observed that the stress value is distributed stably up to 20 mm of bending. However, an increase in the stress ratio is observed in the region where the force acts due to the continuation of bending. This is thought to be due to the folding behavior of the square geometry. The edges of the square-profile geometries support the load in the vertical direction. Therefore, the K side door bars had higher crash criterion values than the S side door bars. In this context, the K5 side door bar provided higher performance than the S5.

Figure 9(b) shows the stress concentrations that occur during bending of the side door bar, code S5, which has a cylindrical external geometry. An examination of Figure 9(b) reveals that the local folding in K5 is now generalized folding in S5. This results in an increase in structural stability and energy absorption. However, although the S5 model resisted deformation, it had a lower SEA value than the K5, suggesting that this may be related to the folding pattern.

An overall evaluation of Figure 9(a-b) reveals that the most significant factor affecting the bending behavior of the multi-cell side door bars is the external geometric shape of the structure. It was determined that the K5 side door bar exhibited localized bending behavior during bending, while the S5 side door bar exhibited folding behavior spread throughout the structure. Based on these results, it was determined that square structural geometries also increase energy absorption because they support the load in a vertical direction.

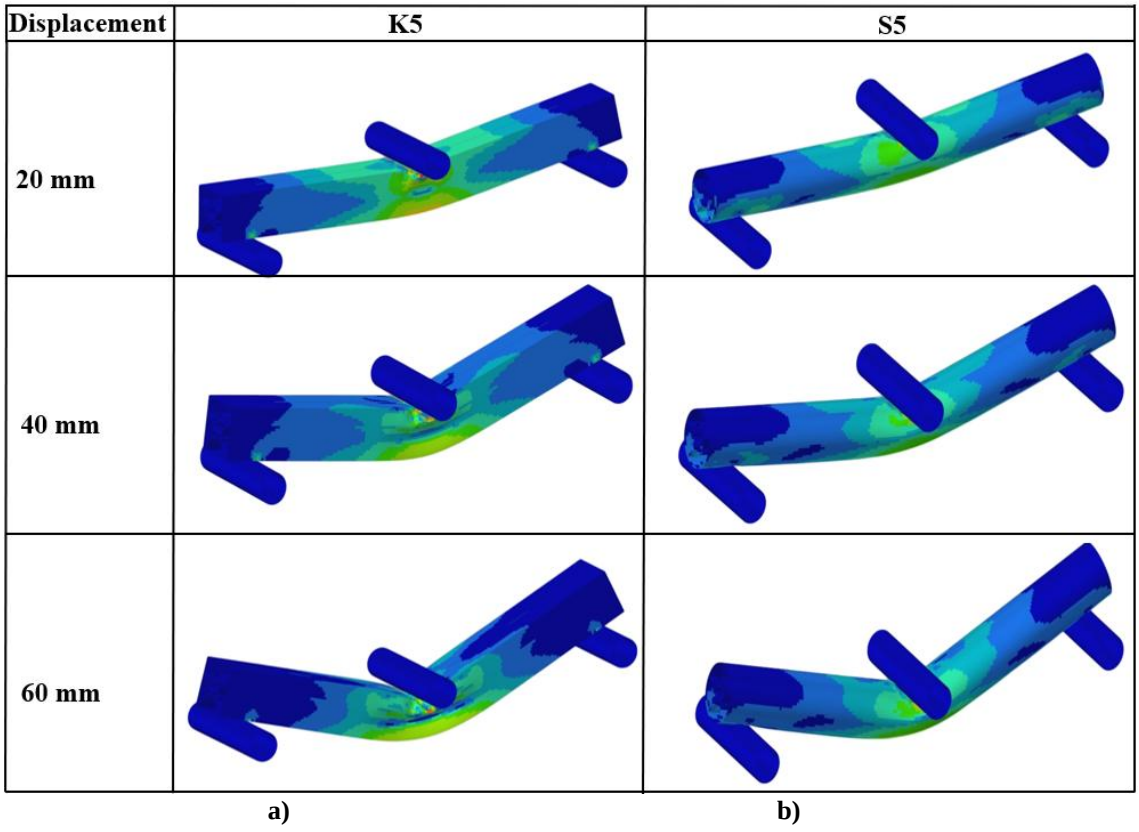

Figure 9. Bending images of side door bars: a) K5 coded design, b) S5 coded design

In vehicle accidents, changes in the direction and center of force acting on the side door bars, the door rigidity, and the impact angle can alter the level of the center openings. These varying loading conditions can alter the initial plastic deformation and local buckling susceptibility, leading to an increase in the PCF value. Based on this information, the K5 side door bar design improved its impact resistance and increased PCF due to stress concentration at the corners.

Consequently, square-section K-models develop dominant plastic hinges at the top and bottom inside corner intersections under three-point bending conditions, where geometric discontinuities lead to the highest stress concentrations. These hinge zones initiate earlier and spread more uniformly across the beam span, resulting in more stable folding behavior and improved EA performance. In contrast, cylindrical S-models exhibit more uniform ovalization and outward shell buckling, resulting in a larger deformation zone but less local stress accumulation. Therefore, the superior vertical load-carrying capacity of square sections is attributed to the restraining effect provided by their rigid corners, which delays the onset of overall buckling and increases the contribution of local plastic deformation to the overall energy absorption capacity.

5. Conclusion

In this study, the K and S series represent side door beams with square and cylindrical cross-sections, respectively. The results obtained in the study are as follows:

- In side door beams with cylindrical cross-sections, the EA, MCF, and SEA values were found to increase with increasing cell numbers. However, despite this increase, the performance of structures with cylindrical cross-sections was observed to be lower than that of square cross-section beam structures with an equal number of cells.
- When the configurations related to square section beams were examined, the five-cell square section beam (K5) structure was the beam structure that best exhibited the EA, MCF and SEA values.
- Since square-section structures effectively carry the load applied in the vertical direction, they exhibit superior load and collision performance compared to cylindrical beam structures.
- Under realistic lateral impact conditions, it is predicted that off-center loading situations can trigger asymmetric bending mechanisms in the structure, leading to increased peak force levels. In particular, in the K5 configuration, it is assessed that the increased rigidity of the corner regions strengthens the structural resistance to oblique impacts; however, stress concentrations in these same regions may lead to an increase in maximum collision force (PCF) values. Accordingly, a systematic investigation considering different impact points and variable loading angles is planned for future studies.

As a result of the study, it was determined that supporting the side door bars with multi-cellular structures will have a positive impact on the energy absorption values. The data obtained from this study will inform future research.

Acknowledgements

The authors declare that this study was conducted without any financial support or institutional funding. No external support was received during the preparation or execution of this research.

References

[1] Tarlochan F. Sandwich structures for energy absorption applications: A review. Materials 2021;14(16):Article 16. doi:10.3390/ma14164731

[2] Yang J, et al. Laser additive manufacturing of bio-inspired metallic structures. Chin J Mech Eng Addit Manuf Front 2022;1(1):100013. doi:10.1016/j.cjmeam.2022.100013

[3] Zhang W, Xu J, Yu TX. Dynamic behaviors of bio-inspired structures: Design, mechanisms, and models. Eng Struct 2022;265:114490. doi:10.1016/j.engstruct.2022.114490

[4] Zou Y, Fu J, Chen Z, Ren L. The effect of microstructure on mechanical properties of corn cob. Micron 2021;146:103070. doi:10.1016/j.micron.2021.103070

[5] Yao SN. Equalization in ambisonics. Appl Acoust 2018;139:129–139. doi:10.1016/j.apacoust.2018.04.027

[6] Yao S, Li Z, Ma W, Xu P. Crashworthiness analysis of a straight-tapered shrink tube. Int J Mech Sci 2019;157–158:512–527. doi:10.1016/j.ijmecsci.2019.04.058

[7] Andrews KRF, England GL, Ghani E. Classification of the axial collapse of cylindrical tubes under quasi-static loading. Int J Mech Sci 1983;25(9):687–696. doi:10.1016/0020-7403(83)90076-0

[8] Kopar M, Yıldız AR. Experimental and numerical investigation of crash performances of additively manufactured novel multi-cell crash box made with CF15PET, PLA, and ABS. Mater Test 2024;66(9):1510–1518. doi:10.1515/mt-2024-0100

[9] Xie S, Jing K, Zhou H, Liu X. Mechanical properties of Nomex honeycomb sandwich panels under dynamic impact. Compos Struct 2020;235:111814. doi:10.1016/j.compstruct.2019.111814

[10] Xu X, Zhang Y, Chen X, Liu Z, Xu Y, Gao Y. Crash behaviors of hierarchical sandwich-walled columns. Int J Mech Sci 2019;161–162:105021. doi:10.1016/j.ijmecsci.2019.105021
[11] Li QQ, Li E, Chen T, Wu L, Wang GQ, He ZC. Improve the frontal crashworthiness of vehicle through the design of front rail. Thin-Walled Struct 2021;162:107588. doi:10.1016/j.tws.2021.107588
[12] Huang Z, Zhang X. Crashworthiness and optimization design of quadruple-cell aluminum/CFRP hybrid tubes under transverse bending. Compos Struct 2020;235:111753. doi:10.1016/j.compstruct.2019.111753
[13] Wang H, Tan D, Liu Z, Yin H, Wen G. On crashworthiness of novel porous structure based on composite TPMS structures. Eng Struct 2022;252:113640. doi:10.1016/j.engstruct.2021.113640
[14] Zhang XW, Zhang QM, Ren XJ. Theoretical study on the dynamic compression and energy absorption of porous materials filled with magneto-rheological fluid. Int J Impact Eng 2022;161:104105. doi:10.1016/j.ijimpeng.2021.104105
[15] Huang L, et al. Bionic composite metamaterials for harvesting of microwave and integration of multifunctionality. Compos Sci Technol 2021;204:108640. doi:10.1016/j.compscitech.2020.108640
[16] Ha NS, Pham TM, Chen W, Hao H, Lu G. Crashworthiness analysis of bio-inspired fractal tree-like multi-cell circular tubes under axial crash. Thin-Walled Struct 2021;169:108315. doi:10.1016/j.tws.2021.108315
[17] Hu J, Luo Y, Liu S. Two-scale concurrent topology optimization method of hierarchical structures with self-connected multiple lattice-material domains. Compos Struct 2021;272:114224. doi:10.1016/j.compstruct.2021.114224
[18] Lucarini S, Cobian L, Voitus A, Segurado J. Adaptation and validation of FFT methods for homogenization of lattice based materials. Comput Methods Appl Mech Eng 2022;388:114223. doi:10.1016/j.cma.2021.114223
[19] Ma W, Li Z, Xie S. Crashworthiness analysis of thin-walled bio-inspired multi-cell corrugated tubes under quasi-static axial loading. Eng Struct 2020;204:110069. doi:10.1016/j.engstruct.2019.110069
[20] Tran T, Hou S, Han X, Chau M. Crash analysis and numerical optimization of angle element structures under axial impact loading. Compos Struct 2015;119:422–435. doi:10.1016/j.compstruct.2014.09.019
[21] Fan Z, Lu G, Liu K. Quasi-static axial compression of thin-walled tubes with different cross-sectional shapes. Eng Struct 2013;55:80–89. doi:10.1016/j.engstruct.2011.09.020
[22] Xiang J, Du J, Li D, Scarpa F. Numerical analysis of the impact resistance in aluminum alloy bi-tubular thin-walled structures designs inspired by beetle elytra. J Mater Sci 2017;52(22):13247–13260. doi:10.1007/s10853-017-1420-z
[23] Kim TH, Reid SR. Bending collapse of thin-walled rectangular section columns. Comput Struct 2001;79(20):1897–1911. doi:10.1016/S0045-7949(01)00089-X
[24] Huang Z, Zhang X. Three-point bending collapse of thin-walled rectangular beams. Int J Mech Sci 2018;144:461–479. doi:10.1016/j.ijmecsci.2018.06.001
[25] Jiang P, Wang Q, Yin A, Hu J, Gu X. Optimization design for foam-filled double cylindrical tubes under multiple lateral impacts. Adv Mech Eng 2018;10(12):1687814018811239. doi:10.1177/1687814018811239
[26] Hwang YH, Han JH. Crashworthiness of energy absorbing structures under combined shear-compression loading: Effects of materials and geometries. Int J Aeronaut Space Sci 2025;26(2):615–628. doi:10.1007/s42405-024-00779-5
[27] H. Taghipoor, A. Eyvazian, F. Musharavati, T. A. Sebaey, ve A. Ghiaskar, "Experimental investigation of the three-point bending properties of sandwich beams with polyurethane foam-filled lattice cores", Structures, c. 28, ss. 424-432, Ara. 2020, doi: 10.1016/j.istruc.2020.08.082.
[28] Gong C, Bai Z, Lv J, Zhang L. Crashworthiness analysis of bionic thin-walled tubes inspired by the evolution laws of plant stems. Thin-Walled Struct 2020;157:107081. doi:10.1016/j.tws.2020.107081
[29] Halis S, Altın M. Numerical investigation of energy absorption performance in thin-walled structure under three-point bending test. Int J Automot Sci Technol 2024;8(1):Article 1. doi:10.30939/ijastech..1434645
[30] Albak Eİ. Optimization for multi-cell thin-walled tubes under quasi-static three-point bending. J Braz Soc Mech Sci Eng 2022;44(5):207. doi:10.1007/s40430-022-03525-8
[31] Zheng D, Zhang J, Lu B, Zhang T. Energy absorption of fully clamped multi-cell square tubes under transverse loading. Thin-Walled Struct 2021;169:108334. doi:10.1016/j.tws.2021.108334
[32] Gliszczyński A, Czechowski L. Collapse of channel section composite profile subjected to bending. Part I: Numerical investigations. Compos Struct 2017;178:383–394. doi:10.1016/j.compstruct.2017.07.033
[33] Zhang X, Fu X. New theoretical models for the bending moment of thin-walled beams under three-point bending. Appl Math Model 2023;121:21–42. doi:10.1016/j.apm.2023.04.015
[34] Huang Z, Zhang X. Three-point bending collapse of thin-walled rectangular beams. Int J Mech Sci 2018;144:461–479. doi:10.1016/j.ijmecsci.2018.06.001
[35] Huang Z, Li Y, Zhang X, Chen W, Fang D. A comparative study on the energy absorption mechanism of aluminum/CFRP hybrid beams under quasi-static and dynamic bending. Thin-Walled Struct 2021;163:107772. doi:10.1016/j.tws.2021.107772
[36] Kim HC, Shin DK, Lee JJ. Characteristics of aluminum/CFRP short square hollow section beam under transverse quasi-static loading. Compos Part B Eng 2013;51:345–358. doi:10.1016/j.compositesb.2013.03.020
[37] Tang Z, Liu S, Zhang Z. Analysis of energy absorption characteristics of cylindrical multi-cell columns. Thin-Walled Struct 2013;62:75–84. doi:10.1016/j.tws.2012.05.019
[38] Chen T, Zhang Y, Lin J, Lu Y. Theoretical analysis and crashworthiness optimization of hybrid multi-cell structures. Thin-Walled Struct 2019;142:116–131. doi:10.1016/j.tws.2019.05.002
[39] Papaiya V, Schuster J, Shaik YP. Development of a side door composite impact beam for the automotive industry. Open J Compos Mater 2024;14(1):Article 1. doi:10.4236/ojcm.2024.141001

[40] Zhang X, Fu X. New theoretical models for the bending moment of thin-walled beams under three-point bending. Appl Math Model 2023;121:21–42. doi:10.1016/j.apm.2023.04.015

[41] O. Gülcan, "Crashworthiness of laser powder bed fusion processed In718 auxetic metamaterials", J. Braz. Soc. Mech. Sci. Eng., c. 46, sy 7, s. 414, Haz. 2024, doi: 10.1007/s40430-024-04927-6.